Chromospheric Heating and CO Simulations

Han Uitenbroek

National Solar Observatory/Sacramento Peak, P.O. Box 62, Sunspot, NM 88349, USA

Abstract. The solar chromosphere is a very dynamic and highly structured environment. In contrast to the higher density hydrodynamically controlled photosphere, this environment is controlled by magnetohydrodynamic forces. The lower density chromosphere encompasses the transition from optically thick to thin so that Non-LTE radiative transfer applies. While the omni-presence of emission in UV lines indicates that a chromospheric rise in temperature from the cool photosphere to the hot corona should occur everywhere on the solar surface, the presence of cool material at chromospheric heights observed in infrared CO lines has made us reconsider the validity of using this interpretation of the observed spectrum based on average one-dimensional models for chromospheric thermal structure. It can be shown that the mean thermal properties of spatially inhomogeneous and/or time-dependent atmospheres in fact are not well represented by an average one-dimensional semi-empirical model based on the mean spectrum. Observations of CO lines show that the coolest locations in the upper photosphere/lower chromosphere are associated with the strong adiabatic expansion that occurs over granules. Simulations that try to model chromospheric dynamics should therefore probably include the effects of solar convection, wave dynamics, as well as the effect of radiative cooling in the multitude of infrared CO lines on the thermal balance of the atmosphere.

1. Introduction

Perhaps the chromosphere is best characterized as the location of the initial rise in temperature from the cool photosphere, where the temperatures in the sun reach their minimum values, to the hot corona, where temperatures reach values comparable to the interior of the Sun. Given the 100% filling factor of the hot coronal gas this rise has to be global, but it does not necessarily occur everywhere at the same height, and it certainly does not occur everywhere under the same physical conditions of pressure, density and temperature. This contribution concentrates on the way observations of CO lines with low brightness temperatures, together with results of recent radiation-hydrodynamics simulations, have forced us to reconsider our traditional ideas of chromospheric structure. Hopefully, new physical models based on these observations and calculations will provide a better framework for understanding the still largely elusive problem
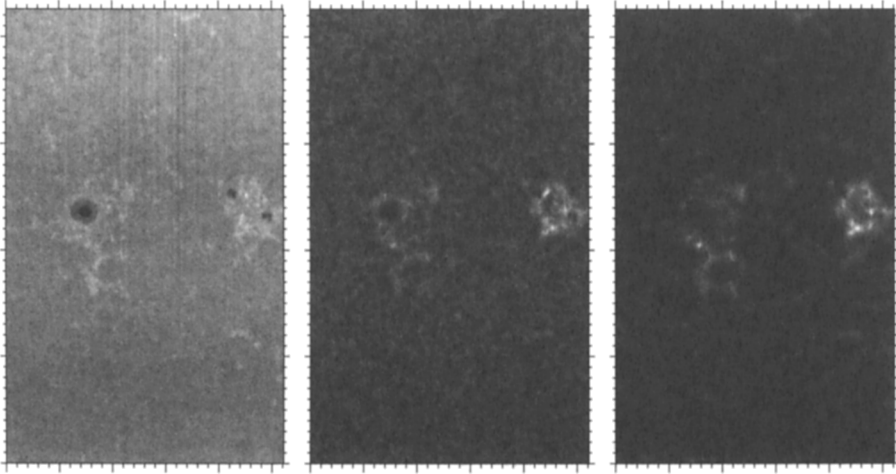
Figure 1.   Successively higher layers of the solar atmosphere are imaged by selecting different wavelengths in the 854.2 nm line ranging from (left to right) outer wing, inner wing and core of the line. Observations were taken with the Kitt Peak Vacuum Tower Telescope.

of chromospheric heating, and will allow us to quantify how much mechanical energy is required to produce the observed chromospheric emission.

Despite many decades of observations, including several decades of UV observations it is remarkable that many details of chromospheric structure still elude us, including the precise mechanism of chromospheric heating. This is both an observational problem as well as a difficulty in modeling. An additional difficulty is the often unacknowledged problem of estimating formation heights of chromospheric lines, which is even more difficult than in the case of the photosphere.

The chromosphere of course, owes its name to the bright crimson emission in the hydrogen H-alpha line, which is only visible when the moon blocks the otherwise dominant and multi-colored emission from the photosphere just before or after totality during an eclipse. When the photospheric light is blocked by selecting only a a small wavelength band centered around the same H-alpha line a very complex picture emerges. This structure is mostly due to the magnetic field and therein lies for a large part the difficulty in studying the chromosphere.

Thus, like the photosphere, the chromosphere is a highly structured and very dynamic environment, but the structure is of a very different nature. When we observe the Sun in wavelengths bands that originate from successively higher layers in the solar atmosphere it is clear that the chromosphere embodies the transition from hydrodynamically dominated to magnetically dominated regimes ($\beta = 8\pi P_{\mathrm{gas}}/B^2$ changes larger than one to smaller than one). As an example, this transition is evident when we look at images in wavelengths that are successively closer to the core of a chromospheric line like the Ca II 854.2 line shown in Figure 1. In addition, the chromosphere is transparent at optical

and IR wavelengths, apart from some strong lines, and becomes optically thick in the continuum only at UV and radio wavelengths. Chromospheric densities are low enough so that radiative transition rates generally dominate over collisional rates. Therefore, Non-Local Thermodynamic Equilibrium (NLTE) radiative transfer is required to model spectral line formation in contrast to the photosphere where the much simpler and computationally more expedient approximation of LTE generally holds. These differences make the chromosphere both hard to observe and interpret, and hard to model theoretically.

2. A word of caution: chromospheric line formation heights

Before we turn to a discussion of CO line formation and its implications for chromospheric structure we take a step back and consider the question of formation heights of chromospheric spectral lines. When we analyze a spectral feature we do not a-priori know the formation height of that feature in the atmosphere. This is the case for photospheric lines and it is even more true for chromospheric spectral lines as we will see below. Figure 2 shows the calculated profile of the chromospheric Ca II 854.2 nm IR triplet line through a standard one-dimensional hydrostatic model of the solar atmosphere (model C of Fontenla, Avrett & Loeser, 1993, hereafter FALC). A byproduct of the radiative transfer
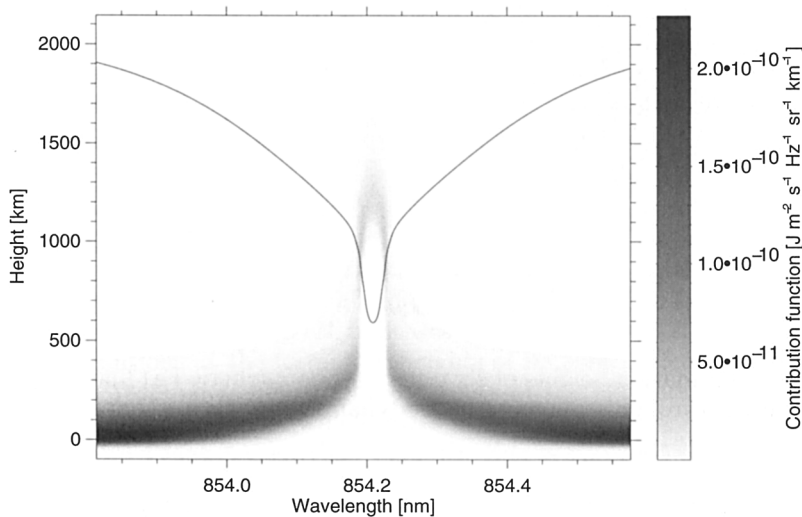
Figure 2. Contribution function to the intensity of the Ca II 854.2 nm line.

calculation is the contribution function, represented by the grey scale map in this figure. It describes for each wavelength in the line where in the atmosphere the intensity at that wavelength comes from. The contribution function can only be calculated if the atmospheric structure is given. Thus, to interpret an observation in the line in term of structure of the atmosphere we have to know

the structure of the atmosphere. In the case of the FALC model the contribu-
tion function shows that the 854.2 line indeed is a chromospheric line as its core
forms at about 1200 km in that model, well above the temperature minimum
region at 500 km.

The real Sun, of course, has spatial structure that is not accounted for
in hydrostatic models like FALC. Dynamic processes, mainly in the form of
(magneto-)hydrodynamics constantly reshape the atmosphere. The correspond-
ing variations and fluctuations in density, temperature, ionization and flow field
profoundly affect the formation heights of spectral lines. This is clearly illus-
trated in Figure 3, which shows the locations of optical depth unity (another
measure of formation height) of six different Fe I lines in a cross section through
a magneto-hydrodynamics simulation snapshot. Clearly, the formation heights
of these photospheric lines are greatly affected by the convection pattern and
are not constant. Indeed the formation heights of individual lines vary by sev-
eral hundred kilometers through the slice, comparable to the range in average
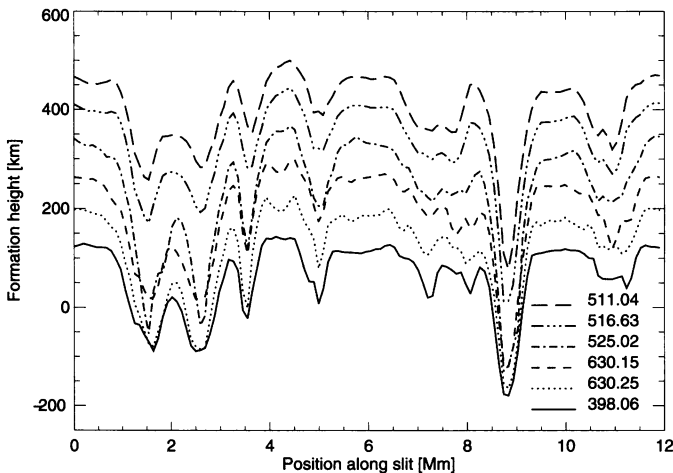formation heights for different lines.

Figure 3.   Formation heights of six different photospheric Fe I lines in
a cross section through a magneto-hydrodynamics simulation snapshot

Chromospheric lines exhibit even larger spreads in their formation heights.
These are strong lines with wings that span in formation height from photosphere
up into the chromosphere. In general these lines also have very steep inner wings,
which can cause the formation height of the intensity at a given wavelength
to shift up and down by as much as 500 km (or equivalently, more than two
chromospheric scale heights) in a macroscopic velocity field. A clear example
is provided by the formation height of the chromospheric Na I D_2 line shown in
Figure 4. The surface plot in this figure represents the ratio of the source function
S in the line to the Planck function B, both at the wavelength indicated in the
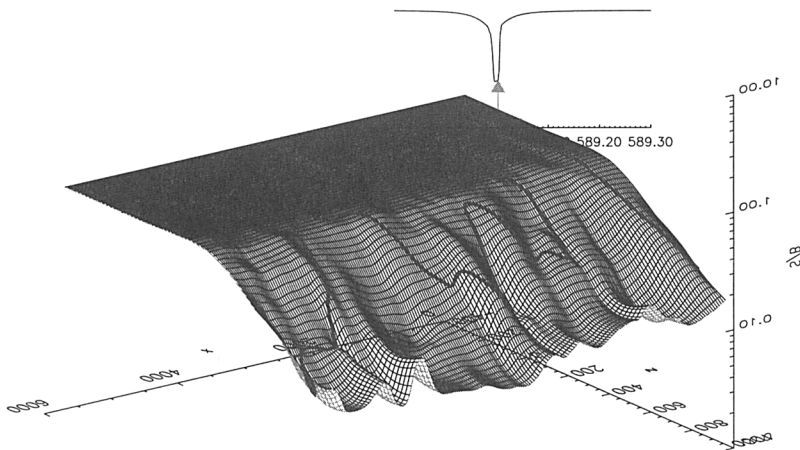inset at the top right, in a cross section through a hydrodynamical simulation

Figure 4.   Surface map of the ratio of the Na I D$_2$ source function S and Planck function B at the wavelength indicated in the inset at top. The thick solid and dashed curves drawn onto the surface mark the location of optical depth unity for the indicated wavelength and the continuum, respectively, in this cross section through a simulation of the solar convection.

of solar convection. The thick solid and dashed lines indicate the position of optical depth unity through the slice of the line plus continuum and continuum only, respectively. The formation height of the Na I D$_2$ intensity at the indicated wavelength thus varies from about 200 km to almost 800 km in the given model. Moreover, the ratio of S/B indicates that the sodium line is decoupled from local conditions at the formation heights of its core. Its core intensity therefore does not respond to the thermodynamics of the chromosphere, in contrast to the continuum intensity, which arises from a layer where $S/B = 1$

Figure 4 makes clear that when the Sun is observed at the indicated wavelength, the signal is a mixture of properties that are encoded at different heights in the atmosphere. It is difficult or impossible to define a single formation height.

3.   Thermal Structure of the Chromosphere

Let us now turn to the thermal structure of the chromosphere. One of the main indicators that the chromospheric temperature rise is a global property of the solar atmosphere is of course the omni presence of UV emission, here exemplified by the full disk spectrum of the OI triplet at 130 nm shown in Figure 5. Likewise, the emission reversals in the Mg II h and k lines indicate that
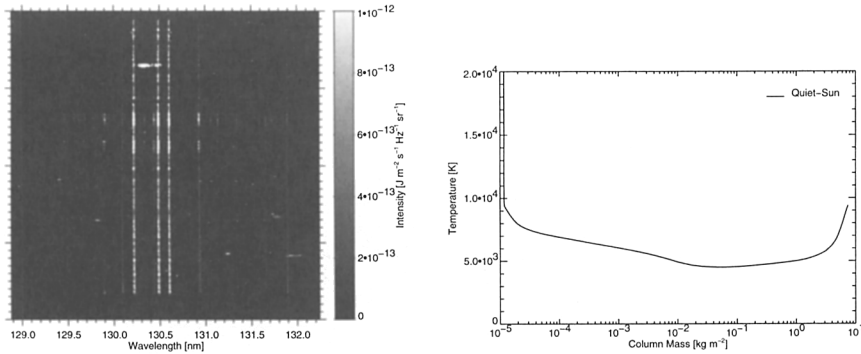
Figure 5.   Full-disk spectrum of the O I triplet at 130 nm observed with the HRTS instrument (left panel, Courtesy K. Dere, NRL). Thermal structure of model FALC (right panel, see text).

a chromospheric temperature rise must occur always and everywhere on the Sun (Uitenbroek, 1997). The same cannot be said, however, about the Ca II H and K lines, which are less opaque by a factor of about ten than the magnesium lines and accordingly form slightly deeper in the atmosphere. The cores of the calcium lines in the quiet Sun show episodes where the emission reversals are completely absent. The emission observed in the UV has prompted solar atmosphere modelers to propose semi-empirical models that have the general structure shown in the right-hand panel of Figure 5 with (from right to left) a temperature decrease in the photosphere, a temperature minimum region and a chromospheric temperature rise towards the hot corona (e.g., model FALC). This simple picture of course stands in stark contrast to the observed complexity of the chromosphere, yet its simplicity is deceiving. A lot of detailed radiative transfer is required to calculate consistently all the Non-LTE ionization departures. But it is a one-dimensional (with variations only in height) semi-empirical in the sense that temperature at each height is adjusted as a free parameter, until the best fit to the average spectrum is achieved.

But the UV emission and Mg II and Ca II line core reversals are not all there is to the chromospheric spectrum. Very contradictory information comes from the CO vibration-rotation lines of the CO molecule in the infrared near 4.7 μm. One may ask what molecular lines have to do with a hot environment like the chromosphere. These lines namely produce dark line cores with brightness temperatures as low as 3700 K when observed close to the limb. Line formation calculations indicate that these lines are very likely in LTE and that these cores form at heights that are above the temperature minimum in classical 1-D models. In the context of one-dimensional hydrostatic models, therefore, these dark cores can only be explained with temperatures that would actually appear at heights in the atmosphere at which one-dimensional hydrostatic models show a chromospheric temperature rise. Instead of the chromospheric temperature rise shown in the righthand panel of Figure 5, the one-dimensional model that reproduces the infrared CO lines (Ayres, Testerman & Brault, 1986). looks like the dashed curve in Figure 6. Thus, it seems impossible to construct a one-
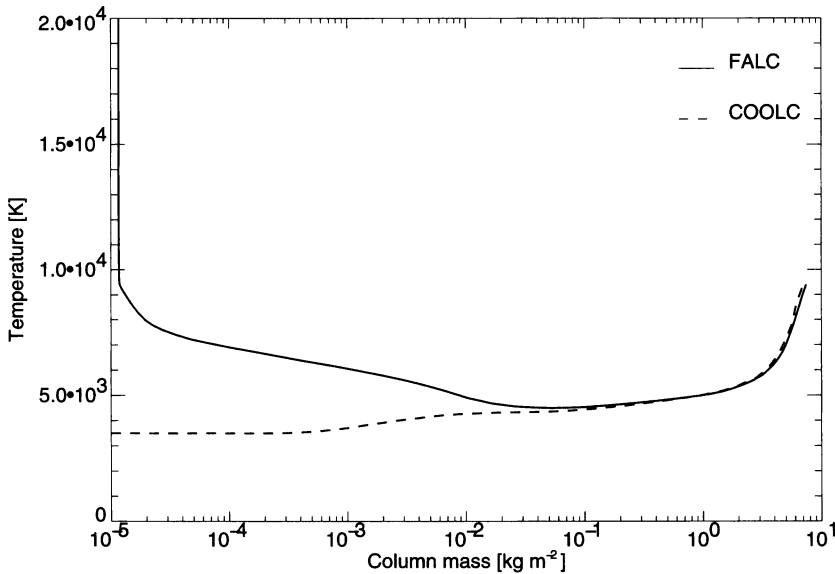
Figure 6. Comparison of of temperature structure of average quiet-Sun model FALC and model COOLC, which reproduces the infrared CO lines.

dimensional model that has a chromospheric temperature rise and is able to explain the dark CO line cores at the same time.

In summary the chromospheric dilemma is the following. Traditional one-dimensional hydrostatic models reproduce the mean chromospheric UV emission spectrum and the shapes of strong lines in the visible fairly accurately. However, they fail to described CO line formation and (obviously) do not deal with inhomogeneities and temporal variability. The question is if they can still be used to accurately describe the radiative losses in the chromosphere, and in particular evaluate its energy balance. Can such models even describe the average properties (like temperature stratification) accurately? These are important questions since radiative loss estimates in stellar models are estimated from 1-D chromospheric models and, similarly, such 1-D models are used for instance as boundary conditions for solar wind calculations.

Indeed, it is straightforward to provide a counter example. Consider a time-dependent atmosphere which reaches minimum temperatures of say 3000 K, but has a mean temperature that is well above 4000 K at every height. Secondly, consider a diagnostic which only has appreciable opacity below 4000 K, and is negligible at higher temperatures. for instance because it ionizes or dissociates This diagnostic will be observable in the average spectrum as it is present in the time-dependent spectrum for at least a fraction of the time. If we try to make a semi-empirical model from the time-averaged spectrum, therefore, we have to conclude (erroneously) that it has a temperature below 4000 K somewhere, or, vice-versa, if we calculate the spectrum through the mean temperature structure

of the time-dependent model the diagnostic will not be present in the calculated spectrum.

4.   The dynamic chromosphere

When viewed in for instance a time series of filtergrams taken in the core of a chromospheric line like Ca II H or K the solar atmosphere appears very dynamic. Waves travel over the surface with typical periods of 3 min and spatial scales of 5″. In the quiet, non-magnetic Sun they are superimposed over a more constant pattern of the solar magnetic network, which shows variations at longer periods of typically 7–10 min. A very characteristic feature of the dynamic behavior of the chromosphere in the quiet Sun is the occurrence of so-called H and K_{2V} grains. These are short trains of transient brightenings of the violet emission reversal in the cores of these lines with typical 3 min periods. The brightenings are preceded by an inner wing brightening, a gradual shift of the K_3 central absorption core to the red, and are followed by an abrupt shift of K_3 to the blue (Rutten & Uitenbroek, 1991). This very specific pattern prompted Carlsson & Stein (1994) to attempt to model the dynamics of the chromosphere with one-dimensional radiation-hydrodynamic simulations. Their
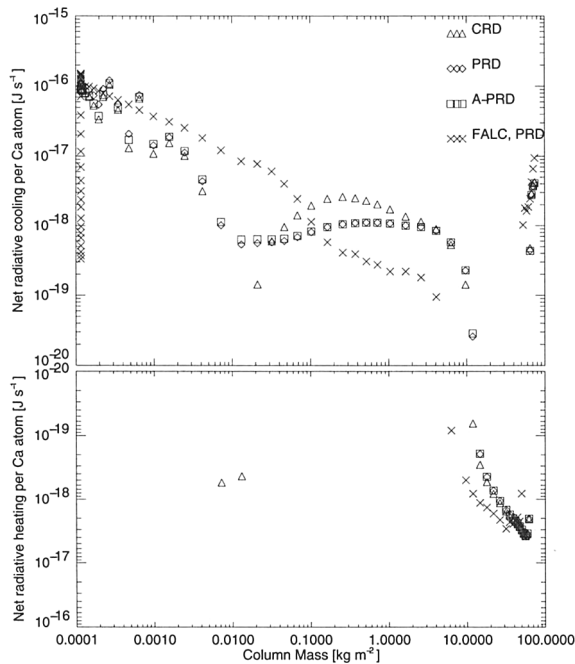

Figure 7.   Radiative losses in the Ca II K line in average quiet Sun model FALC compared with mean average losses in a simulation of chromospheric dynamics.

attempts were very successful in reproducing the K_{2V} brightenings Carlsson & Stein 1997), and moreover, produced simulations of chromospheric dynamics in which the behavior of many more spectral diagnostics can be investigated. Two such investigations are briefly discussed here. First, the effect of the atmosphere's dynamics on the radiative losses in the Ca I K line (the main conduit for radiative energy losses in the solar chromosphere) is discussed, secondly the effect on the formation of the infrared CO lines is discussed.

Radiative loss rates in the Ca I K line under different circumstances are plotted in Figure 7. The triangles, diamonds and squares show the time-averaged radiative losses as a function of column mass over a typical chromospheric oscillation period of 190 sec for complete frequency redistribution (CRD), angle-averaged partial frequency redistribution (PRD), and angle-dependent partial redistribution (A-PRD), respectively (see Uitenbroek, 2002). The crosses denote the radiative losses (scaled to the total number of calcium atoms at each location) for PRD in the hydrostatic FALC model. Clearly the radiative losses calculated in the hydrostatic model differ from the mean radiative losses in the dynamic model, although both models produce the same mean spectrum. Comparing the PRD losses (which most accurately represent reality) the radiative losses are a factor two to three higher in the dynamic case in the low chromosphere and similarly lower in the upper chromosphere. A semi-empirical model built on the average spectrum from the dynamical model, therefore does not accurately predict the actual average radiative losses in the latter.

Uitenbroek (2000b) used the Carlsson & Stein simulations of chromospheric dynamics to investigate the behavior of the infrared CO lines in a dynamic environment. Figure 8 shows the source function at the central wavelength of one of the CO lines at four different times in the simulation. The three down arrows mark the location of optical depths (left to right) 0.3, 1.0 and 3.0, respectively at the indicated wavelength for each time. As time evolves an acoustic disturbance travels up and forms a shock wave when it runs into the more tenuous chromosphere. The heating of the disturbance/shock destroys CO molecules, reduces the opacity in the lines and causes them to form deeper in the atmosphere (times: 60–140 sec). Decompression after the shock (in this case from the shock that passed before the snapshot shown here at time 20 sec) cools the atmosphere and has the opposite effect on the CO line formation. The result of the up and down motion of the CO line formation region is that the line-core intensity varies more than it would if it tracked the temperature variations at one given height like the average formation height. Clearly, when we observe the Sun in a given wavelength in the CO line, we sample different heights in the atmosphere. A time averaged spectrum does not average information encoded at one single height of the atmosphere and this makes the inversion of the mean spectrum in terms of average atmospheric properties a questionable procedure.

Observations show (Uitenbroek 2002) that the observed line core intensities fluctuate by a factor of 2.5 less than predicted by the Carlsson & Stein simulations. One reason may be the assumption of instantaneous chemical equilibrium (ICE) that was used in the CO line formation calculations to calculate the molecular concentrations. It may be that this assumption is no longer valid in a dynamic atmosphere, and that concentrations have to take chemical reaction rates into account. If, for instance, it takes a time comparable to the dynamical

time scales in the atmosphere to form a CO molecules after they are destroyed by a passing shock wave, the concentrations will be less during the cool phases of the atmosphere than assumed under the ICE assumption. However, in a recent paper Asensio Ramos et al. (2003) describe explicit rate calculations of CO formations and conclude that this effect is probably of minor importance for disk center observations. It may be important closer to the limb where shallower, less dense layers of the atmosphere are observed, leading to slower reaction rates.
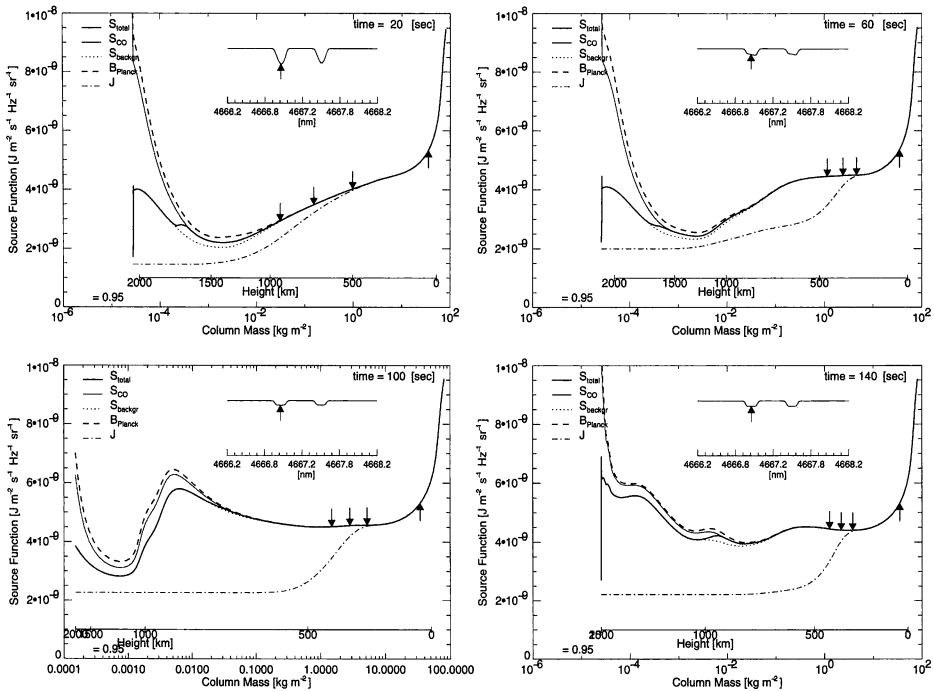

Figure 8.   CO line core source function (solid curves) at three instances in a one-dimensional simulation of chromospheric dynamics. Also plotted are the Planck function at the local instantaneous temperature (dashed curves), the background source function (dotted curves), and mean intensity J (dot-dashed curves). Up arrows mark the location of optical depth 0.3, 1.0, and 3.0 respectively and abound the formation height of intensity at the indicated wavelength.

5.   CO observations

The left panel of Figure 9 shows a spectro-heliogram in the CO 3-4R21 infrared line near 4.7 μm of a quiet solar region obtained under excellent seeing conditions at the McMath-Pierce telescope on Kitt Peak (Uitenbroek, 2000a). Upon close inspection it reveals a pattern that resembles the granulation pattern in the visible but with opposite contrast: granules appear dark while intergranular lanes
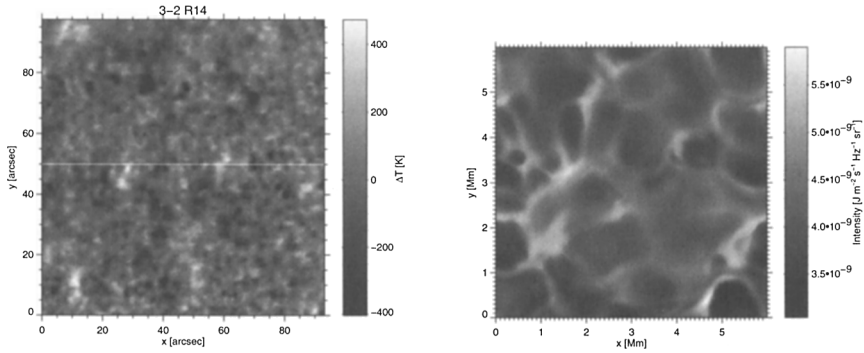
Figure 9. CO spectro-heliogram (left panel) and map of CO line core intensities calculated from a three-dimensional hydrodynamics simulation snapshot (right panel).

appear relatively bright. This is reproduced by the calculated intensity in the core of this CO line in a snapshot from a hydrodynamic simulation of solar convection shown in the right panel of Figure 9 (note the very different spatial scales with $1''$ corresponding to 0.7 Mm). The inverted contrast is the result of the adiabatic cooling that takes place when granular upflows run into the less dense overlying stable layer and have to expand rapidly. Over the intergranular lanes material converges and is heated by compression. Since CO lines form higher than the visible continuum they sample these inverted temperatures rather than the regular temperature contrast in the convective layer. Thus observations and model spectra suggest that the coolest material in the solar photosphere and darkest CO line cores should be found over rapidly expanding granules.

6. Conclusions

Very few spectral diagnostics are available to map the chromosphere and observe its structure and dynamics. Of these most require careful Non-LTE radiative transfer modeling because of the prevailing low density conditions, which make spectral inversions hard to perform. On top of that the chromosphere embodies the transition from a gas pressure dominated to a magnetic force dominated regime. To model its behavior and properly estimate its energy balance will require full Non-LTE magneto-hydrodynamic simulations. An additional observational difficulty is that formation heights of chromospheric lines are even harder to estimate than those of photospheric lines.

We find that one-dimensional hydrostatic models based on time- and space averaged spectra do not give a proper representation of the average thermodynamic structure of the chromosphere. A mean spectrum combines information from different heights through variations of the formation height of intensity at a given wavelength, making the inversion of the mean spectrum in terms of a 1-D stratified atmosphere ambiguous.

The presence of low brightness temperature CO lines in the solar spectrum close to the solar limb has forced us to abandon the classical chromospheric picture the one-dimensional hydrostatic modeling had painted. A chromospheric temperature rise cannot occur always and everywhere at the relatively high densities indicated by these semi-empirical models. Simulations of chromospheric dynamics allow both cool episodes to provide deep CO line cores as well as high temperature episodes to provide UV emission. However, these simulations currently appear still incomplete because they do not reproduce the ubiquitously observed UV emission, nor are they cold enough to reproduce deep enough CO lines.

CO line observations hint that the coolest episodes on the solar atmosphere are associated with granular overshoot. It is therefore likely that we will need three-dimensional simulations of chromospheric dynamics that include effects of convection as well as of acoustic shock formation to properly explain the dual hot and cold character of the chromosphere.

References

Asensio Ramos, A., Trujillo Bueno, J., Carlsson, M., & Cernicharo, J. 2003, ApJ, 588, L61

Ayres, T. R., Testerman, L., & Brault, J. W. 1986, ApJ, 304, 542

Carlsson, M., & Stein, R. F. 1994, in M. Carlsson (ed.), Proceeding of the Oslo mini-workshop on Chromospheric Dynamics, Institute for Theoretical Astrophysics, Oslo, Norway, p. 25

Carlsson, M., & Stein, R. F. 1997, ApJ, 481, 500

Fontenla, J. M., Avrett, E. H., & Loeser, R. 1993, ApJ, 406, 319

Rutten, R. J., & Uitenbroek, H. 1991, Solar Phys., 134, 15

Uitenbroek, H. 1997, Solar Phys., 172, 109

Uitenbroek, H. 2000a, ApJ, 531, 571

Uitenbroek, H. 2000b, ApJ, 536, 481

Uitenbroek, H. 2002, ApJ, 565, 1312